

Dutch Physiology Days 2018

Nederlandse Vereniging voor Fysiologie Dutch Physiology Society



34th Dutch Physiology Days

Physiology, current trends and future challenges

22 and 23 November, 2018

**Bilderberg De Buunderkamp
Wolfheze, The Netherlands**

Dutch Physiology Days 2018

Table of Content

Location and directions	2
Organizing committee & juries	4
Committee.....	4
Jury oral presentation young physiologists.....	4
Physiology, current trends and future challenges	5
Program	6
Thursday 22 November	6
Friday 23 November	7
Abstract oral presentations.....	8

Dutch Physiology Days 2018

Location and directions

Bilderberg Hotel De Buunderkamp
Buunderkamp 8
6874 NC Wolfheze
www.bilderberg.nl/wolfheze/hotel-de-buunderkamp/
Telephone: (+31) 026 48211166

Transportation:

By public transport:

You can take the train to Wolfheze. From Wolfheze Railway station you can take the bus, "Buurtbus" line 589 to Doorwerth. The bus line depart once an hour (08.30, 09.30). The ride will take approximately 3 minutes and from the bus stop it will take a 11 minutes walk to Bilderberg Hotel De Buunderkamp. On your way back, please notice the bus leaves at 15.22 hrs, once an hour). Check www.9292.nl/en# to plan your journey. You can also call a taxi 024-3232000.

By Car:

If you use a navigation system please enter Renkum in place of Wolfheze.

From Rotterdam (A15/A50), 's-Hertogenbosch (A50) and Nijmegen (A73/A50):

Via A50, exit 19 (Renkum).

Follow Oosterbeek (N225, Utrechtseweg).

After 4 km turn left to Wolfheze.

In Wolfheze after the railway turn left (Parallel road).

After 2 km turn right (De Buunderkamp).

You will reach the hotel after 600 m.

From Utrecht (A12), Zwolle (A50/A12) and Oberhausen (A3/A12):

Via A12, exit 25 (Oosterbeek, Wolfheze).

Follow Wolfheze.

In Wolfheze after the railway turn right (Parallelweg).

After 2 km turn right (De Buunderkamp).

You will reach the hotel after 600 m.

At Bilderberg Hotel Buunderkamp you can park your car at their own free parking spaces.

Dutch Physiology Days 2018

The main map shows the location of Bilderberg Hotel De Buunderkamp in Wolfheze. It highlights the A50 highway and nearby roads like N224 and N225. Key locations marked include Oosterbeek, Doorwerth, and Renkum. An inset map shows the broader region around Arnhem, with a red box indicating the area covered by the main map. The inset map shows major roads like the A12, A50, and A15, and nearby towns like Arnhem, Valburg, and Ressen.

BILDERBERG
Hotel
De Buunderkamp
Wolfheze

Buunderkamp 8
6874 NC Wolfheze
T 026 482 11 66
F 026 482 18 98
buunderkamp@bilderberg.nl
www.bilderberg.nl

Why settle for less?

Dutch Physiology Days 2018

Organizing committee & juries

Committee

Prof.dr. M.J. (Mark) Post (chair)
Dr. D. (Daphne) Merkus (Secretary General)
Prof.dr. J.G.J. (Joost) Hoenderop
Dr. R.G. (Regien) Schoemaker
Prof.dr. C.A.C. (Coen) Ottenheijm (Treasurer)
Drs. R. (Rick) Schreurs (Young physiologist)
Drs. E. (Eric) Verschuren (Young physiologist)
Mevr. B. (Bianca) Feenstra
Mevr. V. (Vivian) Schellings

Maastricht University
Erasmus University Rotterdam
Radboud University Medical Center
University of Groningen
Amsterdam UMC
Maastricht University
Radboud University Medical Center
Maastricht University
Maastricht University

Jury oral presentation young physiologists

Prof.dr. J.G.J. (Joost) Hoenderop
Prof.dr. C.A.C. (Coen) Ottenheijm
Dr. R.G. (Regien) Schoemaker

Radboud University Medical Center
Amsterdam UMC
University of Groningen

Dutch Physiology Days 2018

Physiology, current trends and future challenges

Understanding of physiology and physiological practice is the backbone of (bio)medical sciences. It is concept-based, and with the advent of newer biophysical, cellular, and molecular biology tools we are beginning to realise the complexity of multi-state, multi-level operations in the functioning of living cells and organisms. There is an urgent need for innovative development of *in vivo* and *in vitro* experimental models, *in silico* models, and the training of young scientists in the field of Physiology. The study of all these levels of organisation has become highly quantitative and far more detailed. The question many people have asked is whether the physiological sciences is ready to deliver on what is its great challenge of the 21st Century. Conducting research at the forefront of the discipline requires up-to-date knowledge on molecular cellular physiology, organ function and integrative physiology. The Physiology days will provide you with new insights at all these levels and guide you at new possibilities in physiology teaching.

Dutch Physiology Days 2018

Program

Thursday 22 November

9.30-10.00 Registration and Coffee

Morning session

Integrative physiology

10.00-10.40 Lecture Prof. dr. Mat Daemen (Amsterdam UMC)
The Heart Brain Connection

10.40-11.00 Dr. Thijs Eijsvogels (Radboudumc)
Exercise at the extremes: novel insights from cardiac imaging studies

11.00-11.20 Nienke Verzaal (Maastricht University)
Electrical dyssynchrony in patients with repaired tetralogy of fallot may occur in both ventricles

11.20-11.40 Vincent Aengevaeren (Radboudumc)
Can marathon running induce myocardial microdamage?

11.40-12.00 Agnieszka Smoczynska (UMC Utrecht)
Beat-to-beat variation of repolarization predicts imminent ventricular arrhythmias in primary prophylactic ICD patients

Lunch

12.00-13.30 Walking lunch

Afternoon session

Molecular cellular challenges in physiology

13.30-14.10 Lecture Dr. Maarten Rookmaker (UMC Utrecht)
Kidney Organoids

14.10-14.30 Martijn van de Locht (Amsterdam UMC)
Mutations in fast skeletal troponin C (TNNC2) cause contractile dysfunction

14.30-14.50 Eric Verschuren (Radboudumc)
Polycystin-1 regulates renal fluid shear stress-mediated purinergic signaling via pannexin-1 channels

14.50-15.10 Michaela Yuen (Amsterdam UMC)
Leiomodin3 – More than just another thin filament pointed end protein?

15.10-15.30 Coffee break

15.30-15.50 Gijs Franken (Radboudumc)
Identification of novel CNNM2 mutations in hypomagnesemia, seizure, and intellectual disability syndrome

15.50-16.10 Meike Ploeg (Maastricht University)
Mechanical stimulation enhances the differentiation of adult rat cardiac fibroblast to myofibroblasts

16.10-16.30 Jarno Steenhorst (Erasmus MC)
Neonatal pulmonary vascular disease and the right ventricle: a two-pronged, preclinical and clinical approach

16.30-16.50 Marloes van den Berg (Amsterdam UMC)
Positive end-expiratory pressure ventilation induces longitudinal atrophy in diaphragm fibers

Check in at the hotel / Walk in the forest

Key lecture on Physiology

17.30-18.10 Prof. dr. Lucien Engelen (Radboudumc)
The end of intramural healthcare

Diner

18.15 Winter BBQ

Dutch Physiology Days 2018

Program

Friday 23 November

7.00-09.30 Breakfast & check out the hotel

Morning session

Understanding the organ

09.30-10.10 Lecture Dr. Daphne Merkus (Erasmus MC)
Coronary microcirculation in heart failure

10.10-10.30 Josine de Winter (Amsterdam UMC)
Fast skeletal muscle troponin activator tirasemtiv improves in vitro muscle function in the Tg.ACTA^{D286G} nemaline myopathy mouse model

10.30-10.40 Break

10.40-11.00 Vladimír Sobota (Maastricht University)
The acetylcholine-activated potassium current inhibitor XAF-1407 terminates atrial fibrillation in goats

11.00-11.20 Michelle Broekhuizen (Erasmus MC)
A common pathway in placental vascular dysfunction and neonatal pulmonary disease: the kynurenine pathway

11.20-11.40 Lisanne Gommers (Radboudumc)
Low gut microbiota diversity and dietary magnesium intake are associated with the development of PPI-induced hypomagnesemia

11.40-12.00 Valerie van Weperen (UMC Utrecht)
Electrophysiological endpoints differ when comparing the mode of action of highly successful anti-arrhythmic drugs in the chronic atrioventricular block dog model with torsade de pointes arrhythmias

Lunch

12.00-13.30 Lunch buffet

Afternoon session

Physiology in higher education

13.30-14.00 Prof. dr. Harold van Rijen (UMC Utrecht)
Physiology teaching at the UMC Utrecht

14.00-14.30 Dr. Jojanneke Huck (Radboudumc)
Physiology in new Radboudumc curriculum, challenges, developments, results

14.30-15.00 Interactive group session on Physiology teaching
- what can we learn from each other?
- what can we share?

Closure

15.00 Closure and departure

Abstracts oral presentations

ELECTRICAL DYSSYNCHRONY IN PATIENTS WITH REPAIRED TETRALOGY OF FALLOT MAY OCCUR IN BOTH VENTRICLES

Verzaal, NJ¹, Massé, S², Downar, E², Nanthakumar, K², Delhaas, T³, Prinzen, FW¹

¹Departments of Physiology and ³Biomedical Engineering, Maastricht University, Maastricht, The Netherlands

²Department of Cardiology, University Health Network, Toronto, Canada

Background

Tetralogy of Fallot (ToF) patients are surgically corrected at an early age. However, pulmonary stenosis relief and ventricular septal defect closure often create a situation with right ventricular (RV) pressure and/or volume overload and a right bundle branch block (RBBB), conditions which may lead to RV failure and serious arrhythmias. We compared the electrical activation patterns in ToF patients after surgical repair (repaired Tetralogy of Fallot, rToF) with those in patients with left bundle branch block (LBBB) and without right or left bundle branch block (non-BBB).

Methods

In 4 rToF patients and 4 patients with LV ischemia/aneurysm (2 non-BBB and 2 LBBB), extensive electrical mapping was performed during medically indicated open heart surgery on cardiopulmonary bypass. Using an epicardial array (112 electrodes), covering both the LV and RV, mapping was performed during sinus rhythm and during epicardial pacing. Unipolar signals were used to determine local activation times. Activation sequences were visualized using custom-written MATLAB software. Electrical dyssynchrony (DYS) was quantified by means of the 5th to 95th percentile interval of the activation times of the electrodes of the entire heart (BiV), LV or RV, measured from the onset of the QRS complex (SR) or the center of the pace spike (pacing).

Results

The figure shows the activation pattern during SR and pacing in one rToF patient. During SR the BiV DYS was higher in patients with rToF (range: 88-124 ms) and LBBB (116-121 ms) than in non-BBB patients (68-73 ms), indicating a larger dispersion of activation times in the first two groups. As expected, LV DYS was higher in the LBBB patients (110-124 ms) than in the non-BBB patients (35-62), but LV DYS was also elevated in the rToF patients (68-129 ms). The RV DYS seemed to be higher in the rToF patients (59-68 ms) than in the other two groups, (non-BBB 26-62 and LBBB 31-65 ms). Epicardial pacing increased the BiV DYS of the non-BBB (to 103-133 ms) and LBBB group (150-153 ms) to values similar to or higher than those in the rToF group (84-132 ms). Both LV DYS (non-BBB 92-129, rToF 82-133 ms and LBBB 112-127 ms), and RV DYS (non-BBB 70-135 ms, rToF 64-86 ms, LBBB 58-59 ms) became comparable in all groups, indicating similar LV myocardial conduction properties.

Conclusion

This small study suggests that rToF patients display electrical dyssynchrony of not only the RV but also the LV. This LV dyssynchrony is not due to abnormal myocardial conduction properties, implying that it may be related to partial LBBB. Because correction of dyssynchrony in LBBB by biventricular pacing is well known to be beneficial, future studies may focus on investigating how rToF patients may benefit from such pacemaker therapy.

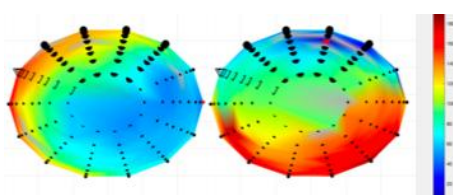


Fig: Example of the epicardial activation pattern during SR (left) and pacing (right) in a patient with rToF. This is a view from the base of the heart, cardiac apex at the center, base at the edges. The LAD (triangles), RV (large spheres) and LV (small spheres) are shown, with activation times represented as colors; blue is early, red is late.

CAN MARATHON RUNNING INDUCE MYOCARDIAL MICRODAMAGE?

Aengevaeren VL¹, Bakermans AJ², Froeling M³, Hopman MTE¹, Hooijmans MT², Monte JR², Strijkers GJ⁴, Nederveen AJ², Eijsvogels TMH¹.

¹Department of Physiology, Radboud University Medical Center, Nijmegen; ²Department of Radiology and Nuclear Medicine, Amsterdam University Medical Centers, University of Amsterdam, Amsterdam, Netherlands;

³Department of Radiology, University Medical Center, Utrecht, the Netherlands; ⁴Biomedical Engineering and Physics, Amsterdam University Medical Centers, University of Amsterdam, Amsterdam, Netherlands.

Background

An acute bout of high-volume high-intensity exercise, such as marathon running, can increase cardiac biomarker concentrations in the blood. It is unknown whether these biomarker elevations are related to myocardial micro-damage. Therefore, we assessed cardiomyocyte damage following a marathon run using cardiac biomarkers and novel magnetic resonance imaging (MRI) techniques including T1, T2 mapping and diffusion tensor imaging (DTI), and subsequently relate cardiac biomarkers to MRI parameters of cardiomyocyte damage.

Methods

Cardiac MRI was performed at 3 Tesla in 12 male participants of the 2017 Amsterdam Marathon during 3 study visits: I) 1 week before, II) 4±2 hrs post-marathon and III) 2 weeks post-marathon. Venous blood samples were collected 1 week before, ~1 hr / ~4 hrs / ~24-48 hrs after finishing the marathon, and 2 weeks after the marathon. We measured cardiac biomarkers (Troponin I, cMyC, sST2), cardiac function (ejection fraction, strain, torsion) and cardiac morphology (volumes, T1 and T2 maps with calculation of extracellular volume fraction, and DTI). DTI allows for an assessment of tissue microstructure through estimates of mean diffusivity and fractional anisotropy, offering a window on cardiomyocyte membrane water permeability and swelling.

Results

11 men (51 [50-56] years) finished the race (42.195km) in 236±35 min at 89±5% of their predicted maximum heart rate. Cardiac biomarkers significantly increased post-exercise, but returned to baseline values 2 weeks post-marathon (troponin I: from 0 [0-0] at baseline to 44 [15-91] at ~1 hr to 57 [16-82] at ~4 hrs to 3 [0-15] at ~24-48 hrs and 0 [0-0] ng/L at 2 weeks after the marathon; cMyC and sST2 showed similar responses). Cardiac ejection fraction and morphology (volumes, T1, T2 maps) did not change following the marathon run (native T1:1214±23 at baseline, 1221±26 4hrs post-marathon and 1206±24 ms 2 weeks post-marathon, p=.15; T2: 50 [48-51] vs. 50 [48-52] vs. 50 [48-52] ms, p=.44). Left ventricular basal strain became less negative from baseline (-25±2%) to post-exercise (-22±2%) and did not completely recover after 2 weeks (-23±3%, p=.003). Extracellular volume fraction (24.6±2.9 vs. 26.5±2.6 vs. 25.0±3.4 %, p=.37), mean diffusivity (1.49±.09 vs.1.60±.16 vs. 1.48±.08 mm²/s, p=.09) and fractional anisotropy (.37 [.33-.39] vs. .38 [.37-.40] vs. .38 [.34-.40], p=.76) did not significantly change post-marathon. Post-exercise troponin was positively associated with changes in mean diffusivity (r=.62, p=.04).

Conclusion

We observed significant elevations in biomarkers of cardiomyocyte damage after marathon running, with a significant association between troponin I and mean diffusivity of myocardial tissue water. Basal strain reduced post-exercise and did not completely return to baseline values after 2 weeks. These findings suggest that cardiac biomarker elevations may result from exercise-induced myocardial micro-damage such as disruption of cardiomyocyte integrity and associated edema. Recovery largely occurred within 2 weeks.

BEAT-TO-BEAT VARIATION OF REPOLARIZATION PREDICTS IMMINENT VENTRICULAR ARRHYTHMIAS IN PRIMARY PROPHYLACTIC ICD PATIENTS

Agnieszka Smoczynska¹, Vera Loen¹, David J. Sprenkeler¹, Mathias Meine², Anton E. Tuinenburg², Henk J. Ritsema van Eck³, Marek Malik⁴, Georg Schmidt⁵, Marc A. Vos¹

¹ Department of Medical Physiology, University Medical Center Utrecht, Utrecht, The Netherlands

² Department of Cardiology, University Medical Center Utrecht, Utrecht, The Netherlands

³ Department of Medical Informatics, Erasmus University Medical Center, Rotterdam, The Netherlands

⁴ National Heart and Lung Institute, Imperial College London, London, United Kingdom

⁵ Medical Klinik und Poliklinik I, Technische Universität München, Klinikum rechts der Isar, München, Germany

Background

Sudden cardiac death (SCD) due to ventricular arrhythmia (VA) is a major healthcare problem, causing approximately 1 in 5 deaths in the Western world. Anti-tachycardia pacing or defibrillation performed by an Implantable Cardioverter-Defibrillator (ICD) has become the mainstay of treatment in the prevention of SCD in patients with ischemic and dilated cardiomyopathy with a left ventricular ejection fraction (LVEF) <35%. Despite being life-saving, ICD therapies are not optimal; they do not prevent VA, and shocks are associated with anxiety and reduced quality of life. Arrhythmic beat-to-beat variation of repolarization quantified as short-term variability (STV) has been proposed as a novel electrophysiological marker for the prediction and prevention of imminent VA in animal models. The aim is to study whether STV of the QT-interval (STV_{QT}) can predict imminent VA in patients.

Methods

High resolution 12-lead Holter recordings of 24 hours were obtained in patients who will receive an ICD for primary prophylaxis, as part of the ongoing EU-CERT-ICD study. Presently available Holters showing >4 consecutive ventricular ectopic beats (EB) were selected. These patients were divided into three groups based on the severity of the arrhythmia: 1) VA lasting <30 seconds and with a heart rate (HR) of <100 beats per minute (bpm) was categorized as slow EB, 2) VA lasting <30 seconds with a HR ≥100 bpm was categorized as non-sustained VA (nsVA), 3) VA lasting ≥30 seconds with a HR ≥100 bpm was classified as sustained VA (sVA). STV_{QT} was determined in lead V2 using the method of fiducial segment averaging and calculated by using the following formula: $\sum |D_{n+1} - D_n| / (N \times \sqrt{2})$, where D_n represents the QT-interval and N is the number of beats. STV_{QT} was determined for 2 minutes prior to VA and at baseline (between 01:30 and 04:30 am).

Results

From the 1544 available Holters, 138 patients were included for analysis. The mean age was 62.8±11.5 years, LVEF was 26.8 ± 5.8%. Ischemic cardiomyopathy was the leading cardiac diagnosis in 58.1% of the patients and the remainder was diagnosed with dilated cardiomyopathy. Overall, STV_{QT} at baseline was 0.88±0.46 ms and increased significantly to 1.11 ± 0.65 ms prior to VA (p<0.0001). STV_{QT} did not increase significantly in patients with slow EBs, from 0.80±0.42 ms at baseline to 1.03±0.51 ms prior to slow EB (p=0.360). However, STV_{QT} did increase significantly in patients with nsVA from 0.89±0.47 ms at baseline to 1.09±0.61 ms prior to nsVA (p=0.030). The increase in STV_{QT} was most pronounced in patients with sVA, from 1.19±0.16 ms at baseline to 2.45±1.20 ms prior to sVA (p=0.004). This rise in STV_{QT} was higher in sVA compared to nsVA (+1.26±1.09 ms vs. +0.19±0.56 ms, p=0.002), and compared to slow EB (+0.23±0.62 ms, p<0.003).

Conclusion

The rise in STV_{QT} predicts imminent VA in patients and that rise correlates with the severity of VA.

MUTATIONS IN FAST SKELETAL TROPONIN C (TNNC2) CAUSE CONTRACTILE DYSFUNCTION

Martijn van de Locht¹, Josine M. de Winter¹, Stefan Conijn¹, Weikang Ma², Michiel H.B. Helmes^{1,3}, Tom C. Irving², Sandra Donkervoort⁴, Payam Mohassel⁴, Livija Medne⁵, Colin Quinn⁶, Osorio L.A. Neto⁴, Steven Moore⁴, A. Reghan Foley⁴, Nicol C. Voermans⁷, Carsten G. Bönnemann⁴, Coen A.C. Ottenheijm¹.

¹ Department of Physiology, VU University Medical Centre, Amsterdam, The Netherlands;

² Biophysics Collaborative Access Team, Center for Synchrotron Radiation Research and Instrumentation, and Department of Biological Sciences, Illinois Institute of Technology, Chicago, Illinois, USA;

³ IonOptix LLC., Milton, MA, USA;

⁴ Neuromuscular and Neurogenetics Disorders of Childhood Section, Neurogenetics Branch, National Institutes of Neurological Disorders and Stroke, National Institutes of Health, Bethesda, MD, USA;

⁵ Roberts Individualized Medical Genetics Center, Children's Hospital of Philadelphia, Philadelphia, Pennsylvania, USA

⁶ Department of Neurology, University of Pennsylvania, Philadelphia, PA, USA

⁷ Department of Neurology, Radboud University Medical Centre, Nijmegen, Netherlands.

Nemaline myopathy (NEM) is a group of rare muscle diseases caused by mutations in genes encoding proteins associated with the thin filament. However, not all thin filament myopathies manifest with characteristic nemaline rods and the spectrum of clinical manifestations is expanding. Troponin C (TnC) binds to TnT and TnI to form the Tn-complex, which regulates thin filament activation. To date, fast skeletal (fs)TnC has not been implicated in disease. Here, we investigate muscle biopsies of two patients with heterozygous, predicted to be damaging mutations (Patient 1 (P1), 27 yrs: c.100G>T; p.Asp34Tyr & patient 2 (P2), 19 yrs: c.237G>C; p.Met79Ile) in the gene encoding fsTnC (TNNC2), manifesting clinically as a unique congenital myopathy. P1 had congenital weakness and vocal cord paralysis requiring tracheostomy, with ptosis, ophthalmoplegia, osteopenia and clinical improvement over time. Also, a brother, mother and maternal grandmother, presenting with similar symptoms were found to carry the TNNC2 mutation. P2 has a milder phenotype, with early respiratory weakness, dysphagia and generalized hypotonia, which improved with age, resulting in normal ambulation with mild proximal weakness at age 19. To investigate the mechanism underlying muscle weakness, we performed contractility measurements on single muscle fibers isolated from patient (N=2) and control (N=5) biopsies. Permeabilized fibers were activated by exogenous calcium. P1 showed atrophied type II and hypertrophied type I fibers (confirmed by histochemical analysis). Absolute and normalized maximal force was decreased in type II and increased in type I fibers. The calcium-sensitivity of force was decreased in type II and increased in type I fibers. P2 showed similar results but less pronounced: a lower decrease in calcium-sensitivity of force in type II fibers, no loss of maximal force and no atrophy in type II fibers. In P1, low angle X-ray diffraction data suggested a compressed thin filament in both fiber types, as suggested by shortening of the actin layer line 6 reflection. X-ray data from P2 showed less pronounced changes.

Conclusion

Based on these findings, we propose that the TNNC2 mutations reduce the calcium sensitivity of force, presumably due to changes in thin filament structure, contributing to muscle weakness in patients. The more severe clinical phenotype of P1 compared to P2 is reflected in the experimental results.

POLYCYSTIN-1 REGULATES RENAL FLUID SHEAR STRESS-MEDIATED PURINERGIC SIGNALING VIA PANNEXIN-1 CHANNELS

Eric H.J. Verschuren¹, Juan P. Rigalli¹, Charlotte Castenmiller¹, Joost G.J. Hoenderop¹, Dorien J.M. Peters², René J.M. Bindels¹, Francisco J. Arjona¹

¹Department of Physiology, Radboud university medical center, the Netherlands

²Department of Human Genetics, Leiden University Medical Center, the Netherlands

Background

The *Pkd1* gene encodes polycystin-1 (PC1), a mechanosensor for urinary flow that triggers intracellular responses in kidney tubular cells. Mutations in *Pkd1* lead to polycystic kidney disease (PKD), a major cause of renal failure. In PKD, ATP might play an important role in disease progression. ATP is released from renal epithelial cells when exposed to fluid shear stress (FSS). In this study, the role of PC1 in FSS-mediated purinergic signaling was assessed.

Methods

Wildtype, *Ift140*^{-/-} (lacking primary cilia) and *Pkd1*^{-/-} mDCT15 cells, generated via CRISPR/Cas9 technology, were used. Cells were exposed to fluid flow in μ -slide I^{0.4}/IV^{0.4} channels, yielding physiological FSS of 0.3, 0.6 and 1.2 dyn/cm². ATP released by the cells and in the urine of *Pkd1*^{-/-} mice was measured using a luciferase assay. Cells were incubated with 100 μ M BB-FCF or 100 μ M rapamycin to assess the involvement of pannexin-1 and mTORC1, respectively, in ATP release. Gene expression relevant to purinergic signaling was assessed using real-time quantitative PCR.

Results

Exposure of wildtype and *Ift140*^{-/-} mDCT15 cells to 0.3, 0.6 and 1.2 dyn/cm² FSS displayed a significant FSS-magnitude dependent ATP release. In *Pkd1*^{-/-} mDCT15 cells this magnitude dependent effect was not observed, however, ATP release at 0.3 dyn/cm² FSS was significantly higher than in wildtype mDCT15 cells. Urinary ATP release and *Panx1* expression in pre-cystic *Pkd1*^{-/-} mice was significantly increased as compared to wildtype mice. FSS-mediated ATP release was significantly inhibited when mDCT15 cells were exposed to BB-FCF in both wildtype and *Pkd1*^{-/-} conditions. FSS-mediated ATP release by wildtype mDCT15 cells exposed to rapamycin was significantly amplified, this effect was absent in *Pkd1*^{-/-} mDCT15 cells. Furthermore, expression of *Panx1*, *P2ry1*, *P2rx5*, *Entpd2* and *Entpd3* was significantly increased in wildtype mDCT15 cells after 3-hour exposure to 0.6 dyn/cm² FSS.

Conclusion

Our data illustrate that PC1 regulates FSS-activated ATP release, independently of the presence of primary cilia. This release is amplified by mTORC1 inhibition and mediated by pannexin-1 channels. Thus, pannexin-1 is proposed as a potential novel therapeutic target in PKD.

LEIOMODIN3 - MORE THAN JUST ANOTHER THIN FILAMENT POINTED END PROTEIN?

Michaela Yuen^{1,2}, Lauren Schultz³, Rachel Mayfield³, Shen Shengy³, Stefan Conijn¹, Irene De Vries¹, Robbert van der Pijl³, Henk Granzier³, Carol Gregorio³, Coen A. C. Ottenheijm^{1,3}

¹Department of Physiology, Institute for Cardiovascular Research, Amsterdam UMC (Location VUmc), Amsterdam, the Netherlands

²Discipline of Paediatrics and Child Health, Faculty of Medicine, University of Sydney, Sydney, Australia

³Department of Cellular and Molecular Medicine, University of Arizona, Tucson, USA

Background

Leiomodlin-3 (LMOD3), encoded by *LMOD3*, is a newly discovered protein in striated muscle which localises predominantly near the thin contractile filament pointed end in the centre of the muscle sarcomere. *LMOD3* mutations cause a severe skeletal muscle myopathy characterised by neonatal death due to respiratory insufficiency. The severity of disease and the presence of abnormal thin filaments in patient muscle suggest that an important role of LMOD3 in skeletal muscle likely by helping to form and maintain thin filaments. Despite LMOD3 being critical for muscle biology, to date, little is known about LMOD3s *in vivo* role and the pathophysiology of *LMOD3*-related disease.

Methods

We characterised pathological changes in *Lmod3* knock-out (KO) mouse muscle by performing immunohistological analysis in skeletal muscle from *Lmod3* KO mice and litter mate controls. Furthermore, we determined whether LMOD3 is directly involved in skeletal muscle stability and contraction by testing the structural integrity and contractile function of intact soleus muscle and permeabilised single myofibres.

Results

We found a selective atrophy of fast 2B fibres in *Lmod3* KO mouse muscle and a shift towards slower type 2a and type 1 myofibres. Eccentric “damaging” contractions resulted in less force loss in KO mice compared to littermate controls, suggesting muscle integrity is not affected by LMOD3 loss. Interestingly, permeabilised single myofibres showed reduced cross bridge cycling speed specifically in fast 2a myofibres.

Conclusion

The presented study suggests that LMOD3 loss may have distinct effects in various skeletal muscle fibre types. While the slowest fibre type (type 1 fibres) seem relatively spared, LMOD3 loss results in 2B fibre atrophy and abnormal contractile dynamics in fast 2a myofibres. LMOD proteins have previously been suggested to predominantly regulate actin filament formation and length similar to other proteins that localise to the thin filament pointed ends. Our study suggests LMOD3 plays a more complex role in skeletal muscle and may directly affect skeletal muscle cross bridge cycling, perhaps by regulating myosin-actin interactions. Future studies will focus on the exact mechanism by which LMOD3 modulates cross bridge cycling and if this may contribute to skeletal muscle dysfunction in *LMOD3*-myopathy patients.

IDENTIFICATION OF NOVEL CNNM2 MUTATIONS IN HYPOMAGNESEMIA, SEIZURE, AND INTELLECTUAL DISABILITY SYNDROME

Gijs A.C. Franken, Femke Latta, Joost G.J. Hoenderop, René J.M. Bindels, Jeroen H.F. de Baaij

Department of Physiology, Radboud Institute for Molecular Life Sciences (RIMLS), Radboud university medical center (Radboudumc), Nijmegen, the Netherlands

Background

Cyclin M2 (CNNM2) is a transmembrane protein which is essential for extrusion of Mg^{2+} from the renal epithelial cells towards the blood compartment in the kidney. It is exclusively expressed in the distal convoluted tubule of the nephron, which is responsible for 10% of Mg^{2+} reabsorption from the pro-urine in the kidney. Mutations found in CNNM2 are known to cause the hypomagnesemia, seizures, and intellectual disability (HSMR) syndrome, a rare congenital disorder. In this study, the largest cohort of novel HSMR patients to date is described and functionally characterised.

Methods

To study the effects of the novel identified mutations on CNNM2 function, human embryonic kidney 293 (HEK293) cells overexpressing normal or mutant CNNM2 were investigated. Firstly, the stable isotope $^{25}Mg^{2+}$ was used to assess CNNM2-regulated/mediated Mg^{2+} -transport. In addition, cell surface biotinylation and immunocytochemistry were performed to study the localisation of CNNM2 of wild type or mutant CNNM2.

Results

Patients carrying CNNM2 mutations typically had significantly low serum Mg^{2+} levels, ranging from 0.48 to 0.70 mM (normal range: 0.7-1.1 mmol/L), and intellectual disability. Manifestations were observed at birth or early in childhood. Patients treated with magnesium supplementation had only a limited increase in serum Mg^{2+} concentrations. The identified CNNM2 mutations were found in the signal peptide domain, the helical domain, the extracellular loop, and the intracellular domain. Among the mutations, there were six amino acid substitutions, one single residue deletion, and three large truncations. Out of nine tested CNNM2 mutations, seven showed a significant loss of function regarding their $^{25}Mg^{2+}$ uptake capacity ranging from approximately 50-95%. Investigation of the protein expression by the cell surface expression assays and confocal microscopy revealed that deletions and mutations in the signal peptide domain significantly decreased cell surface expression.

Conclusion

The data presented showed that many identified CNNM2 mutations are causative for the HSMR syndrome in this patient cohort. Here, we underline the significance of CNNM2 in maintaining Mg^{2+} homeostasis and the importance of functional testing for accurate diagnosis of HSMR syndrome. However, how these mutations link to intellectual disability has yet to be elucidated and needs further investigation.

MECHANICAL STIMULATION ENHANCES THE DIFFERENTIATION OF ADULT RAT CARDIAC FIBROBLAST TO MYOFIBROBLASTS

M.C. Ploeg, C. Munts, M. van Bilsen, F.W. Prinzen, F.A. van Nieuwenhoven

Department of Physiology, Cardiovascular Research Institute Maastricht (CARIM), Maastricht University, Maastricht, The Netherlands

Background

Cardiac fibroblasts (CFs) play an important role in the healing process after myocardial infarction. During this healing process, CFs can differentiate into myofibroblasts, a process that is characterized by increased expression of contractile proteins such as alpha-smooth muscle actin (α SMA) and structural extracellular matrix (ECM) proteins, such as collagens. In addition, CF differentiation induces changes in the expression of many non-structural ECM proteins (matricellular proteins), such as connective tissue growth factor (CTGF), Tenascin C (TNC), and Cartilage intermediate layer protein-1 (CILP-1) playing various roles in ECM homeostasis. It is acknowledged that growth factors such as Transforming growth factor beta (TGF β) play an important role in the process of CF differentiation. Aside from changes in biochemical factors influencing CF in the healing infarct, many changes in tissue properties and remodeling will affect the mechanical signaling in CF. We investigated to what extent myofibroblast differentiation is influenced by mechanical loading conditions.

Methods

Primary rat CFs were cultured on flexible silicon membranes and mechanically stimulated by cyclic stretch at 1 Hz (Flexcell system). The standard stretch protocol consisted of 10% cyclic stretch for 5h or 24h. In a subset of experiments, during the 5h protocol, after 1h, stretch was alternated for 1h no stretch (interrupting stretch) or 1h 20% cyclic stretch (increasing stretch). Gene expression analysis was performed by qPCR, measuring the expression of genes involved in myofibroblast differentiation (α SMA, TGF β , CTGF, TNC, and CILP-1). Cyclophilin was used as a control gene for normalization. All experiments were performed with cells from ($n \geq 6$) separate CF isolations and expression differences were tested by paired t-test.

Results

After 5h of cyclic stretch, gene expression of TGF β and TNC was increased (1.6-fold and 2.1-fold respectively, both $p < 0.01$). After 24h of cyclic stretch, gene expression of TGF β was again increased together with α SMA and CTGF (1.7-fold; 1.6-fold; and 1.4-fold respectively, all $p < 0.01$). Gene expression of CILP-1 was decreased (2.9-fold $p < 0.01$) after 24h of cyclic stretch. Both interrupting and increasing stretch to 20% for 1h resulted in a (non-significant) 1.2-fold increase in expression of TGF β compared to 10% stretch.

Conclusion

Cyclic stretch stimulates differentiation of CF to myofibroblasts, as evidenced by increased expression of α SMA. This differentiation appears to be triggered/mediated by early increases in TNC and TGF β , whereas a slower increase in the expression of CTGF and a decrease in the expression of CILP-1 also play a role. Future experiments will focus on further elucidating the effect of intermittent changes in stretch in CFs (comparable to variable loading conditions in the in vivo heart).

NEONATAL PULMONARY VASCULAR DISEASE AND THE RIGHT VENTRICLE: A TWO-PRONGED, PRECLINICAL AND CLINICAL APPROACH

J.J. Steenhorst^{1,3}, A. Hirsch^{2,3}, W.A. Helbing^{3,4}, I.K.M. Reiss⁵, D. Merkus¹

¹ Department of Cardiology, Division of Experimental Cardiology, ErasmusMC Rotterdam, The Netherlands.

² Department of Cardiology, Division of Cardiology, ErasmusMC Rotterdam, The Netherlands

³ Department of Radiology, Division of Radiology and Nuclear Medicine, ErasmusMC Rotterdam, The Netherlands

⁴ Department of Pediatrics, Division of Pediatric Cardiology, ErasmusMC Rotterdam, The Netherlands

⁵ Department of Pediatrics, Division of Neonatology, ErasmusMC Rotterdam, The Netherlands

Background

Neonatal pulmonary vascular disease (PVD) is a common co-morbidity in several neonatal pathologies, with bronchopulmonary dysplasia (BPD) in very or extreme preterm born infants (gestational age (GA) <32 weeks) as most prevalent cause. If progression into pulmonary hypertension (PH) occurs, mortality rates up to 40% before two years of age have been reported, mostly by deterioration into right ventricular failure. Unfortunately, a cure does not exist and underlying mechanisms and clinical features of patients who progress into PH and right ventricular failure are poorly understood. Furthermore, after recovery, pulmonary arterial pressure normalizes, while maximal exercise tolerance is limited into young adulthood. Other long-term consequences for the pulmonary vasculature and right ventricle as a result of early exposure to PVD are currently unknown, including contributions of risk factors later in life such as aging, western diet, hypertension, pregnancy or metabolic derangement.

For this purpose, we propose a two-pronged approach; 1) a preclinical approach in which we will develop a swine model for neonatal PH. This enables us to study disease severity, progress, mechanisms, (long-term) consequences, exercise tolerance and possible treatments in a large animal model with similar hemodynamics as humans. 2) a clinical approach in which we will set up a follow-up study for young adult survivors of bronchopulmonary dysplasia, the population at risk for neonatal PVD, to investigate long-term pulmonary and cardiac consequences.

Preclinical approach

Previously, in our laboratory, transient PH in neonatal piglets was produced with use of hypoxia (4wk) with right ventricular remodeling. However, this model was associated with high mortality (40% before wk4). Here, we propose a symptom-guided adaptation to this model to limit mortality. Again, animals will be exposed to hypoxia or normoxia (Sham) shortly after birth. Using weekly echocardiograms under sedation, a scoring system consisting of echocardiographic parameters of disease progress and presence of clinical symptoms will be developed to guide return to normoxia. In addition, weekly blood samples may contribute to early detection using biomarkers of disease progress. Following hypoxia, piglets will recover for 4 weeks in normoxia. Subsequent after recovery, piglets are chronically instrumented with catheters. One week after surgery, exercise-treadmill-training commences, allowing continuous measurements of pressures and cardiac output at rest and during exercise at different levels of intensity. At follow-up (3mnd), heart and lung tissue will be harvested for histological and molecular analyses.

Clinical approach

Young adult survivors of prematurity with BPD (born GA<30 wks), survivors of prematurity without BPD (born GA<30 wks) and at term born controls (born GA>37 wks), will perform several pulmonary function tests and a cardiopulmonary exercise test. Furthermore, cardiac structure and function of the subjects at rest and during physiological stress will be investigated, using echocardiography and exercise cardiac Magnetic Resonance Imaging (cMRI).

(Expected) Results

At this point, we have successfully overcome problems associated with exercising in the MRI. The protocol for the cMRI has been optimized and consists of a baseline scan, several levels of exercise intensity followed by a real-time sequence.

The two-pronged approach proposed here enables us to investigate mechanisms and perform interventional studies to prevent, postpone, arrest or to reverse PVD or right ventricular maladaptation in a neonatal swine model, but also investigate long-term consequences in BPD survivors. In the future, the model might be suited to introduce risk factors and co-morbidities and might, in combination with the clinical data, reveal patient groups at risk for early pulmonary vasculature or right ventricle pathology later in life.

POSITIVE END-EXPIRATORY PRESSURE VENTILATION INDUCES LONGITUDINAL ATROPHY IN DIAPHRAGM FIBERS

M. van den Berg, MD^{1*}; J. Lindqvist, PhD^{2*}; R. van der Pijl^{1,2}; P. Hooijman, PhD¹; A. Beishuizen, MD, PhD³; J. Elshof, B.Sc⁴; M. de Waard, PhD⁴; A. Girbes, MD, PhD⁴; A. Spoelstra-de Man, MD, PhD⁴; Z. Shi, MD, PhD^{4,5}; C. van den Brom, PhD⁶; S. Bogaards, B.Sc¹; S. Shen, PhD²; J. Strom, PhD²; H. Granzier, PhD²; J. Kole¹; R. Musters, PhD¹; M. Paul, MD, PhD⁷; L. Heunks, MD, PhD⁴; C. Ottenheijm, PhD^{1,2}

¹ Dept Physiology, ⁴Intensive Care, ⁶Anesthesiology; ⁷Cardiothoracic Surgery, Amsterdam UMC, Location VUmc, Amsterdam, the Netherlands; ²Dept of Cellular and Molecular Medicine, University of Arizona, Tucson, USA; ³Dept of Intensive Care, Medisch Spectrum Twente, Enschede, the Netherlands; ⁵Dept of Critical Care Medicine, Beijing Tiantan Hospital, Capital Medical University, Beijing, PR China. *: both authors contributed equally.

Background

Critically ill patients often develop diaphragm weakness, which prolongs ventilator dependency, hospital stay, and increases mortality and health care costs. Mechanisms underlying diaphragm weakness include cross-sectional atrophy and contractile dysfunction of diaphragm muscle fibers, but whether shortening of these fibers (*i.e. longitudinal atrophy*) occurs is unknown.

Objectives

To study the hypotheses that: (1) an increased end-expiratory lung volume during positive end-expiratory pressure (PEEP) ventilation causes caudal diaphragm displacement and acute shortening of diaphragm fibers; (2) diaphragm fibers adapt to this acutely shortened position by reducing their contractile filament lengths or the number of serially-linked sarcomeres – the smallest contractile units in the muscle – to maintain a maximum force generating capacity; (3) adaptation is modulated by the giant mechanosensing protein titin.

Methods

Diaphragm displacement, visualized by ultrasound, and diaphragm fiber shortening during different levels of PEEP ventilation were examined in critically ill patients and shortly mechanically ventilated wild type rats. Diaphragm fiber adaptation during long-term PEEP ventilation was studied in critically ill patients and 18h mechanically ventilated wild type rats. Modulatory effects of titin were assessed in 18h mechanically ventilated wild type rats and rats with a more compliant titin isoform (RBM20 deficient rats).

Results

This study shows that (1) in patients PEEP ventilation results in 0.40 ± 0.10 cm and 0.89 ± 0.17 cm caudal diaphragm displacement at $\Delta 5$ and $\Delta 10$ cmH₂O PEEP; in rats PEEP ventilation results in 0.24mm displacement per cmH₂O PEEP. In rats, acute displacement caused by 2.5 cmH₂O PEEP was accompanied by shorter full-length diaphragm fibers (18.0 ± 0.5 vs. 19.9 ± 0.4 mm; $p=0.01$), and shorter sarcomere lengths (2.64 ± 0.06 vs. 2.85 ± 0.07 μm; $p=0.04$) at end-expiration. (2) After long-term PEEP ventilation, diaphragm fibers in rats adapted to the shorter sarcomere length by reducing the number of serially-linked sarcomeres by 12% (5488 ± 128 vs. 6250 ± 170 ; $p=0.004$), whereas contractile filament lengths did not change. (3) RBM20 deficient rats did not show a reduced number of serially-linked sarcomeres after 18h of PEEP ventilation (PEEP vs. control: 7005 ± 777 vs. 7155 ± 424 ; $p=0.70$).

Conclusion

Diaphragm fibers show longitudinal atrophy during PEEP ventilation, which might be modulated by titin-borne elasticity. We postulate that longitudinal atrophy contributes to a lower force generating capacity of the diaphragm during spontaneous breathing trials in critically ill patients. During these trials PEEP and the end-expiratory lung volume are reduced, which stretches the shortened diaphragm fibers to excessive sarcomere lengths. At these longer sarcomere lengths, muscle fibers generate less force and diaphragm weakness ensues.

FAST SKELETAL MUSCLE TROPONIN ACTIVATOR TIRASEMTIV IMPROVES IN VITRO MUSCLE FUNCTION IN THE Tg.ACTA1^{D286G} NEMALINE MYOPATHY MOUSE MODEL

JM de Winter^{1*}, TC Borsboom^{1*}, E Minardi², C Gineste³, DT Hwee⁴, FI Malik⁴, KJ Nowak^{5,6}, J Gondin^{3,7}, MA Pellegrino², R Bottinelli², CAC Ottenheijm¹

* contributed equally

¹ VU University medical center, Amsterdam, The Netherlands

² Department of Molecular Medicine, Pavia University, Pavia, Italy

³ Aix Marseille Univ, CNRS, CRMBM, Marseille, France

⁴ Research and Early Development, Cytokinetics, Inc., South San Francisco, California, United States

⁵ Centre for Medical Research, Faculty of Health and Medical Sciences, The University of Western Australia, and Harry Perkins Institute of Medical Research, Nedlands, Western Australia.

⁶ Office of Population Health Genomics, Division of Public and Aboriginal Health, Department of Health, Western Australia.

⁷ Institut NeuroMyoGène, UMR CNRS 5310 – INSERM U1217, Université Claude Bernard Lyon 1, Villeurbanne, France

Background

Nemaline myopathy (NM) results in muscle weakness results and a poor quality of life. We evaluated the acute effect of *tirasemtiv* – a fast skeletal muscle troponin activator - on *in vitro* extensor digitorum longus (EDL) muscle mechanics in the skeletal muscle α -actin-based NM mouse model (Tg.ACTA1^{D286G}, n=14) and wildtype mice (Wt, n=14).

Methods

Intact muscle preparations were stimulated at incremental frequencies in both the absence and presence of *tirasemtiv* (3 μ M). Fiber cross-sectional area (CSA) was determined by histology.

Results

Tg.ACTA1^{D286G} mice had lower EDL muscle weights (Tg.ACTA1^{D286G}: 9 \pm 0.3 mg vs. Wt: 12 \pm 0.4 mg, P <0.001) and muscle fiber CSA (Tg.ACTA1^{D286G}: 1251 \pm 45 μ m² vs. Wt: 1650 \pm 116 μ m², P =0.03). Absolute force production was lower in Tg.ACTA1^{D286G} mice. Administration of *tirasemtiv* (3 μ M) restored absolute force levels at submaximal stimulation to those of Wt mice (20 Hz: Tg.ACTA1^{D286G}-vehicle: 25 \pm 3 mN, Wt-vehicle: 35 \pm 3 mN (P =0.03), Tg.ACTA1^{D286G}-*tirasemtiv*: 42 \pm 5 mN; 40 Hz: Tg.ACTA1^{D286G}-vehicle: 40 \pm 5 mN, Wt-vehicle: 64 \pm 8 mN (P =0.02), Tg.ACTA1^{D286G}-*tirasemtiv*: 76 \pm 10 mN).

Conclusion

These findings are pivotal steps towards a therapeutic strategy to combat muscle weakness in NM.

THE ACETYLCHOLINE-ACTIVATED POTASSIUM CURRENT INHIBITOR XAF-1407 TERMINATES ATRIAL FIBRILLATION IN GOATS

Vladimír Sobota, Giulia Gatta, Marion Kuiper, Arne van Hunnik, Ulrich Schotten, Sander Verheule
Department of Physiology, Cardiovascular Research Institute Maastricht, Maastricht, The Netherlands

Background

Atrial fibrillation (AF) is the most common sustained cardiac arrhythmia, occurring in 1-2% of the population. Currently available antiarrhythmic drugs for treatment of AF are often ineffective and have side-effects, including ventricular proarrhythmia. The acetylcholine-activated potassium current (I_{KACH}) has been proposed as a promising atrial-selective target for AF treatment. This study investigates the effect of I_{KACH} inhibition in goat using a selective I_{KACH} blocker XAF-1407.

Methods

Six Dutch milk goats (55±6 kg) were used. The animals were instrumented with pericardial electrodes for sensing and stimulation. Two weeks after the implantation surgery, stimulation protocols in awake animals were performed (normal atria). Atrial effective refractory periods were measured during the administration of two doses of XAF-1407: 0.3 and 3.0 mg/kg. The measurements were repeated after 2 days of AF (electrically remodelled atria), maintained by burst pacing. Subsequently, after a period of recovery from remodelling (>5 days) AF was induced again and maintained for 3 weeks. Cardioversion experiments with XAF-1407 (dose of 0.3 mg/kg followed by 3.0 mg/kg) were performed after 2 weeks of AF maintenance, using vernakalant (dose of 3.7 mg/kg followed by 4.5 mg/kg) as active control. Each dose was administered using a loading dose lasting for 20 minutes, followed by a maintenance dose of another 20 minutes. The order of the experiments was randomized, yielding the same average day after the start of AF induction.

Results

Significant prolongation of the aERP was observed during administration of XAF-1407 in both normal and electrically remodelled atria, as shown in the table.

Table 1: Changes in electrophysiological parameters. The data are presented in milliseconds (mean±SD).

Parameter	Cycle length	Normal atria			Electrically remodelled atria		
		Baseline	0.3 mg/kg	3.0 mg/kg	Baseline	0.3 mg/kg	3.0 mg/kg
QRS		48±8	49±6	53±7	49±3	52±4	54±7
QT	400	258±2	259±4	274±10	259±9	260±6	276±22
aERP	400	149±26	181±28	226±32	73±17	115±9	167±27
	250	154±5	169±8	187±6	91±13	121±7	154±7

A small prolongation of mean QRS and QT was observed after administration of 3 mg/kg in normal atria as well as in electrically remodelled atria. Infusion of XAF-1407 resulted in cardioversion in 5 out of 6 goats with an average time to cardioversion of 42±27 min. Compared to that, 4 out of 6 animals cardioverted during infusion of vernakalant with an average time to cardioversion of 63±12 min. No ventricular proarrhythmic event (extrasystoles, non-sustained VT) was observed during administration of either vernakalant or XAF-1407.

Conclusion

Our study indicates that XAF-1407 is a potent atrial-selective drug for AF cardioversion.

A COMMON PATHWAY IN PLACENTAL VASCULAR DYSFUNCTION AND NEONATAL PULMONARY DISEASE: THE KYNURENINE PATHWAY

Michelle Broekhuizen^{1,2,3}, Zongye Cai³, Daphne Merkus³, A.H. Jan Danser², Irwin K.M. Reiss¹

¹Department of Pediatrics; Division of Neonatology, Erasmus MC University Medical Center, Rotterdam, the Netherlands, ²Department of Internal Medicine; Division of Pharmacology and Vascular Medicine, Erasmus MC University Medical Center, Rotterdam, the Netherlands, ³Department of Cardiology; Division of Experimental Cardiology, Erasmus MC University Medical Center, Rotterdam, the Netherlands

Background

Pregnancy diseases such as pre-eclampsia (PE) often lead to foetal growth restriction and pre-term birth with severe consequences, including bronchopulmonary dysplasia and neonatal pulmonary hypertension (PH). Pregnancy-related diseases are proposed to be a consequence of impaired placental vascular development, evidenced by inflammation and microvascular remodelling, which are also hallmarks of PH. The placental and pulmonary vasculature both contain the only microvasculatures that constricts to hypoxia and displays endothelial expression of indolamine 2,3-deoxygenase (IDO1). IDO1 is the rate limiting enzyme in the metabolism of tryptophan to kynurenine along the kynurenine pathway (KP). In the placenta specifically, the KP is believed to aid in foeto-maternal tolerance. Moreover, kynurenine, as well as other tryptophan metabolites, are vasoactive. Since microvascular dysfunction and decreased IDO1 expression are present in both placental and pulmonary disease, we hypothesize that decreased IDO1 expression may be a common detrimental pathway in these pathologies. We therefore aim to investigate the role of alterations in the KP in vascular placental (dys)function and hypoperfusion. Secondly, we aim to study the potential of KP metabolites to mediate and/or act as biomarker for development of neonatal pulmonary vascular diseases.

Methods

Placentas were collected within 30 minutes after caesarean section, from woman with either uncomplicated pregnancies (n=12) or PE (BP >140/90 mmHg and proteinuria, n=7 early onset PE, n=4 late onset PE), and biopsies from both the maternal and foetal side were snap frozen. Gene expression of all enzymes of the KP was determined by RT-qPCR on both the maternal and foetal side of the placenta. In addition, IDO1 expression was also measured by RT-qPCR in pulmonary autopsy material from infants with neonatal PH as well as controls, obtained from the Pathology department. In future experiments, metabolites will be determined by LC/MS in both maternal and foetal blood, and linked to clinical outcome of the baby. The effect of tryptophan metabolism on vasoreactivity will be studied in an ex-vivo dual sided placental perfusion set-up, and wire-myography experiments.

Results

IDO1 was the most prominently expressed enzyme of the KP in the placenta. This enzyme was expressed higher on the foetal side compared to the maternal side of the placenta in both control and early onset PE, samples from late onset PE showed a similar trend. IDO1 expression was lower in early onset, but not late onset PE as compared to healthy pregnancies. In contrast, arylformamidase, the enzyme that follows up on IDO1 in the KP, and converts N-formyl-kynurenine into kynurenine, was upregulated in early-onset PE. The enzyme 3-hydroxyanthranate oxygenase, converting 3-hydroxy-athranilate to quinolinate, was downregulated in both early onset and late onset PE. In the lungs of infants with neonatal PH IDO1 was also downregulated.

Conclusion

The reduced expression of IDO1 in early onset, but not late onset PE, suggests a different pathological process in both diseases. The KP, and potentially IDO1 specifically, might provide a link between pregnancy related pathologies, and infant BPD and PH. Identification of this link and the mechanism of development of these diseases may reveal novel therapeutic targets.

LOW GUT MICROBIOTA DIVERSITY AND DIETARY MAGNESIUM INTAKE ARE ASSOCIATED WITH THE DEVELOPMENT OF PPI-INDUCED HYPOMAGNESEMIA

Lisanne M.M. Gommers¹, Thomas H.A. Ederveen^{2,3}, Jenny van der Wijst¹, Caro Overmars-Bos¹, Jos Boekhorst^{2,3}, René J.M. Bindels¹, Jeroen H.F. de Baaij¹, and Joost G.J. Hoenderop¹

¹ Department of Physiology, Radboud Institute for Molecular Life Sciences (RIMLS), Radboud university medical center (Radboudumc), Nijmegen, The Netherlands.

² Center for Molecular and Biomolecular Informatics (CMBI), RIMLS, Radboudumc, Nijmegen, The Netherlands.

³ NIZO, Ede, The Netherlands.

Background

Proton pump inhibitors (PPIs) are used by millions of patients for the treatment of stomach acid-related diseases. Although PPIs are generally considered safe, about 13% of the users develops hypomagnesemia. Despite rising attention for this issue, the underlying mechanism is still unknown. Here, we aim to examine whether the gut microbiome is involved in the development of PPI-induced hypomagnesemia.

Methods

To assess the effects of the PPI omeprazole on magnesium (Mg^{2+}) homeostasis and gut microbiota, wild-type C57BL/6J mice were treated daily with 20 mg/kg bodyweight omeprazole for four weeks under normal or low dietary Mg^{2+} availability. Subsequently, Mg^{2+} homeostasis was assessed by means of serum, urine and fecal electrolyte measurements and gut microbiota composition was investigated by 16S rRNA gene sequencing.

Results

Omeprazole significantly reduced serum Mg^{2+} levels on the low Mg^{2+} diet (1.20 ± 0.05 vs. 1.05 ± 0.05) without affecting the mRNA expression of *Trpm6* and *Trpm7* in colon or kidney. Overall, these mice showed a lower gut microbial diversity in response to omeprazole treatment. Redundancy analysis identified a shift in microbial composition in omeprazole-treated mice compared to controls. In particular the abundance of *Lactobacillus* and *Bifidobacterium* was increased with 3-fold and 2-fold, respectively. To examine the metabolic consequences of the microbial alterations, the colonic composition of organic acids was further evaluated. Low dietary Mg^{2+} intake, independent of omeprazole treatment, resulted in a 10-fold increase in formate levels.

Conclusion

Our study demonstrated that omeprazole treatment alters the gut microbial composition. Additionally, low dietary Mg^{2+} intake affects the metabolic potential of the gut bacteria. Together, these results imply that both omeprazole treatment and low dietary Mg^{2+} intake disturb the gut lumen environment and may pose a risk for the malabsorption of Mg^{2+} in the colon. Given the widespread use of PPIs, not only serum Mg^{2+} levels but also dietary Mg^{2+} intake and microbiome status should be closely monitored by healthcare practitioners.

ELECTROPHYSIOLOGICAL ENDPOINTS DIFFER WHEN COMPARING THE MODE OF ACTION OF HIGHLY SUCCESSFUL ANTI-ARRHYTHMIC DRUGS IN THE CHRONIC ATRIOVENTRICULAR BLOCK DOG MODEL WITH TORSADE DE POINTES ARRHYTHMIAS

V.Y.H. van Weperen, A. Bossu, V.J.A. Bourgonje, M.B. Thomsen, A. Oros, H.D.M. Beekman, M.A. Vos
Department of Medical Physiology, University Medical Center Utrecht, Utrecht, The Netherlands.

Background

Torsade de Pointes arrhythmias (TdP) in the anaesthetized, chronic atrioventricular block (CAVB) dog are believed to ensue from an increase in temporal dispersion of repolarization, favoring the development of ventricular ectopic beats and TdP that stop spontaneously or require cardioversion. Accordingly, parameters such as QTc, action potential duration and short-term variability (STV) are commonly used to reflect (in)stability of ventricular repolarization in, for example, pharmacology safety screenings. However, this does not take into account the role of spatial dispersion in the perpetuation of TdP. We studied the adequacy of these parameters to accurately display the efficacy of 5 antiarrhythmic drugs capable of suppressing drug-induced TdP in >80% of the experiments.

Methods

The effects of flunarizine (2mg/kg/2'; n = 10; F), verapamil (0.06mg/kg/5', n = 4; V), SEA0400 (0.8mg/kg/5' ; n = 4; S) and GS967 (0.1mg/kg/5' ; n = 7; G) were evaluated following a proarrhythmic challenge (dofetilide 25µg/kg/5'). Electrophysiological recordings included QTc and/or endocardial left ventricular monophasic action potential duration (LV MAPD) and STV. In 5 additional G experiments, spatial dispersion was assessed by intramural mapping of ventricular repolarization using transmural needle electrodes. Severity of arrhythmic events was quantified as arrhythmic score (AS).

Results

The proarrhythmic drugs prolonged the QTc and LV MAPD in all experiments, but only F fully and significantly reversed this effect to baseline values (from +39 and +25 to +3 and +4% of baseline values, respectively). F, V and S decreased the STV convincingly and, except for S, significantly. However, following G the STV remained significantly increased (+245% of baseline values), despite the decrease in AS from 46.7 ± 27.9 to 2.3 ± 1.4 (not significant). This anti-arrhythmic effect was reflected by a significant reduction in spatial dispersion from +280 to +100% of baseline values.

Conclusion

Temporal and spatial dispersion seem to be separately involved in ventricular arrhythmogenesis, as demonstrated by the antiarrhythmic modes of action of the interventions.